applied sciences

MDPI

Article

Study on the Effect of Temperature on the Alignment of a Long-Span Steel–Concrete Composite Beam Track Cable-Stayed Bridge

Xiaogang Li [1,*], Xiangsheng Huang [1], Peng Ding [2], Xiaohu Chen [2], Qiansong Wang [1] and Sihan Cen [1]

[1] School of Civil and Hydraulic Engineering, Chongqing University of Science and Technology, Chongqing 400074, China; 2022206095@cqust.edu.cn (X.H.); 13618333005@163.com (Q.W.); 2023206091@cqust.edu.cn (S.C.)

[2] T. Y. Lin International Engineering Consulting (China) Co., Ltd., Chongqing 401121, China; dingpeng@tylin.com.cn (P.D.); chenxiaohu@tylin.com.cn (X.C.)

* Correspondence: 2021058@cqust.edu.cn; Tel.: +86-135-9409-4526

Abstract: In order to study the effect of temperature on the alignment of a long-span special track bridge, this paper provides a theoretical basis and technical support for bridge design, construction and later operation. This research established the section model of the steel-hybrid beam by COMSOL, and the internal temperature field, transverse temperature, and vertical temperature gradient were analyzed. The Midas Civil bridge model analysis system was established to investigate the influence of temperature difference and temperature gradient on the vertical deformation of the whole bridge. Based on the temperature and displacement monitoring system of the Chongqing Nanjimen track bridge, the temperature and displacement data in 2023 were obtained for comparative analysis. The results show that the temperature field inside the composite beam presents a nonlinear distribution, the daily temperature difference can reach 26.0 °C, and there is a significant temperature gradient between the steel beam and the concrete. The highest temperature is 60.3 °C at 15:00 when the temperature difference between the upper and lower edges of the concrete slab is 11.1 °C, and the daily transverse temperature gradient is 3.2 °C, 5.3 °C and 7.4 °C, respectively. Under the temperature difference in the system, the maximum displacement of the main beam is 92.3 mm, and the mid-span displacement is 132.1 mm under the positive temperature difference. Based on the measured data for the whole year, it is found that the displacement of the main beam under the combined action of ambient temperature and solar radiation significantly exceeds the influence of a single temperature. The research shows that temperature change has an important impact on the stability and durability of the bridge, and temperature monitoring and management should be strengthened in the design and operation stage to ensure the bridge's safety and smooth operation of the train.

Keywords: temperature effect; steel–concrete composite beam; track cable-stayed bridge; bridge alignment

Citation: Li, X.; Huang, X.; Ding, P.; Chen, X.; Wang, Q.; Cen, S. Study on the Effect of Temperature on the Alignment of a Long-Span Steel–Concrete Composite Beam Track Cable-Stayed Bridge. *Appl. Sci.* **2024**, *14*, 10688. https://doi.org/10.3390/app142210688

Academic Editor: Muhammad Junaid Munir

Received: 4 November 2024
Revised: 14 November 2024
Accepted: 17 November 2024
Published: 19 November 2024

1. Introduction

The implementation of the transportation power strategy has facilitated the rapid development of urban rail transit, with the construction of track bridges now well underway. Cable-stayed bridges are widely used in track bridges because of their mature construction technology and beautiful shape [1]. On the other hand, steel–concrete composite beams (SCCBs) have excellent tensile properties of steel and excellent compressive properties of concrete, showing good mechanical properties and durability. SCCB can not only bear large loads but also effectively resist deformation and fatigue, ensuring long-term stable operation of the structure [2–5]. This structural compound and superior physical properties make SCCB an important choice for cable-stayed track bridges [6,7].

High temperature gradients in combination with high levels of restraint may lead to thermal cracking and durability problems in concrete members [8]. In certain instances, the temperature stress exceeds the live load, causing an adverse change in the bridge alignment. The alignment of the bridge floor is the main expression of the overall mechanical performance of the bridge structure, and also an important symbol to measure the overall stiffness of the bridge, which seriously affects the smoothness of the track and the safety and comfort of the traffic [9]. As a high-order statically indefinite structure, the cable-stayed bridge has a significant temperature effect [10], especially for the track cable-stayed bridge in the form of steel-hybrid beams. Due to the specific heat capacities of steel and concrete, steel rises and cools faster, resulting in more prominent problems of temperature stress and deformation [11–13]. Track bridges have narrow widths and high vibration requirements compared to highway and railway bridges. Due to the large traffic volume, high operation frequency, strong load action, and obvious structural response, the alignment change response of the bridge under the action of temperature is more significant [14].

Considering the influence of temperature on cable-stayed bridge alignment, scholars from domestic and international academic institutions have conducted invaluable research. Based on the analysis of the causes of temperature stress, Zhou Hao et al. [15] analyzed the distribution law of the sunshine temperature field and proposed a calculation model combining the vertical temperature gradient of beams and bridge towers and the temperature difference between the cable and bridge towers and main beams. Zhou Yi et al. [16,17] studied the influence mechanism of temperature on the vertical displacement of twin-tower cable-stayed bridges through plane geometry and finite element analysis. They revealed the behavior rule of cable-stayed bridges under the action of temperature. Yang Jingnan et al. [18] analyzed the longitudinal and transverse displacements of the bridge tower caused by temperature, as well as the longitudinal vertical displacements and longitudinal stresses of the main beam in the asphalt paving process, and found that there were large displacements and stress differences in both the longitudinal and transverse parts of the structure, resulting in uncoordinated deformation and excessive local stress. Based on long-term monitoring data, Huang Qiao et al. [19] studied the characteristics of the daily temperature effect under the action of solar radiation and found that the daily temperature effect had seasonal differences in the annual cycle and lagged relative to solar radiation in the daily cycle. Liu Yufei et al. [20] took the concrete-filled steel tube bridge tower as the experimental object, comprehensively considered the influence of the temperature field, and carried out the cavitation measurement. Based on the exposure test, they verified the finite element model and realized the calculation and prediction of the temperature effect before the bridge construction and form. Zhao Yu et al. [21] established a finite element model of the bridge structure and analyzed the effects of system temperature difference, sunshine temperature difference, and cable beam (tower) temperature difference on the deflection of the bridge tower, the alignment of the main beam, and cable force. Based on the half-year temperature monitoring data of the ballastless track site, C compared and analyzed the variation characteristics of temperature and temperature gradient in the CRTS II plate ballastless track based on a simply supported box girder, roadbed and bridge transition section, and found that the non-Gaussian and non-stationarity of temperature in the ballastless track on the transition section were more significant within half a year, and the non-Gaussian property on the roadbed was the worst. To sum up, scholars at home and abroad have conducted extensive, in-depth research on the temperature effect of bridges. Furthermore, scholars at home and abroad have carried out beneficial exploration of the influence of temperature on bridge alignment and bridge temperature effect. However, there are only a few researches on track bridges, especially on the special form of steel composite beam. Therefore, it is necessary to study the influence of temperature on the linear shape of the superimposed beam cable-stayed track bridge. It is expected to provide more targeted solutions for the safety design and maintenance of such special bridges, filling the gaps in the current research field, and providing substantial guidance for future engineering practice.

In view of this, this research establishes a section model of the steel–concrete composite beams (SCCBs) based on COMSOL6.2, studies their temperature field distributions under the mechanism of solar radiation, convective radiation, and heat conduction, and analyzes the temperature gradient distribution inside the composite beam and the transverse temperature distribution on the upper, middle and lower edges of the concrete slab and inside the steel beam. Then, the numerical simulation model of the whole bridge was established by Midas Civil 2023 to analyze the vertical deformation of the whole bridge under the action of temperature difference and temperature gradient of the system and to analyze the influence of temperature action on the bridge alignment. Finally, based on the temperature and deformation monitoring system of the Chongqing Nanjimen track bridge, the field-measured temperature and transverse and vertical deformation were collected for analysis, and the influence of temperature on the alignment of long-span steel-hybrid beam track cable-stayed bridge was obtained, which provided technical support for the comfort and safety of driving and a scientific basis for the healthy maintenance of the bridge.

2. Experimental

2.1. Basic Principle of Structural Temperature Field

- Heat conduction.

According to the basic principles of thermodynamics, temperature transfer is always from high temperature to low temperature. For any point in the structure, its temperature is a three-dimensional function of time change. According to Fourier's heat conduction theory, the general form of the three-dimensional transient heat conduction differential equation of the structure is obtained [23,24]:

$$\lambda\left(\frac{\partial^2 \mathrm{T}}{\partial x^2}+\frac{\partial^2 \mathrm{T}}{\partial y^2}+\frac{\partial^2 \mathrm{T}}{\partial z^2}\right)=c\gamma\frac{\partial \mathrm{T}}{\partial t}+Q \tag{1}$$

where γ is the density of the material, kg/m^3; c is the specific heat of the material, J/(kg·K); λ is the thermal conductivity, W/(m·K); T is the temperature of any point (x, y, z); t is time, s; Q is the internal heat source intensity, W/m^3.

The cross-sectional variation in SCCB along the longitudinal bridge is not obvious, and the heat conduction along the bridge axis can be ignored. Therefore, the sunshine temperature field of the composite beam can be simplified as a two-dimensional transient temperature without an internal heat source, as shown in Equation (2):

$$\rho c\frac{\partial T}{\partial t}=\lambda\left(\frac{\partial^2 T}{\partial x^2}+\frac{\partial^2 T}{\partial y^2}\right) \tag{2}$$

- Convective heat transfer.

Convective heat transfer is heat exchange between a solid surface and its surrounding fluid due to temperature differences. The factors affecting the heat convection intensity include the contact area between the media, the properties of the media, the flow velocity, the flow space size, the structure, and the fluid temperature. According to Newton's law, heat transfer is proportional to the contact area and temperature difference in the structure [25]:

$$q_c=h_f(T_S-T_B) \tag{3}$$

where q_c is heat transfer, W/m^2; h_f is the convective heat transfer coefficient; T_S is atmospheric surface temperature; T_B is bridge structure surface temperature.

- Thermal radiation.

Radiant heat transfer occurs between objects of different temperatures, when the temperature of the system is consistent, the radiant heat transfer is still in progress, but in a

state of dynamic equilibrium. The radiant heat transfer between the two systems can be calculated using the Steffen–Boltzmann equation [26,27]:

$$h_r = \sigma\varepsilon\left[(T_S + 273.15)^2 + (T_B + 273.15)^2\right](T_S + T_B + 546.3) \quad (4)$$

where ε is the emissivity of the actual object, whose value is always less than 1; σ is the Steffen–Boltzmann constant, whose value is 5.67×10^{-8} w/m^2.

- System temperature difference.

According to GBT51234-2017 Urban Rail Transit Bridge Design Code [28], the temperature difference in the system should be calculated from the closing time of the structure, and the difference between the closing temperature and the extreme minimum temperature and extreme maximum temperature over the years should be taken, respectively [28]

$$\begin{cases} \Delta T_1 = T_{H_1} - T_{L_1} \\ \Delta T_2 = T_{H_2} - T_{L_2} \end{cases} \quad (5)$$

where ΔT_1 and ΔT_2 are, respectively, the overall temperature rise difference, °C; T_{H_1} and T_{H_2} are, respectively, the extreme maximum temperature in the past year and the maximum temperature during the closing, °C; T_{L_1} and T_{L_2} are the lowest temperature and the extreme minimum temperature during the closing in the past years, °C.

- Temperature gradient.

Temperature gradient refers to the change in temperature per unit length in a certain direction in space. It describes the spatial change rate of the temperature field, and its calculation formula is as follows [28].

$$\nabla T = \frac{\Delta T}{\Delta L} \quad (6)$$

where ∇T represents the temperature gradient, ΔT is the temperature difference, and ΔL is the change in spatial position.

2.2. Finite Element Analysis

2.2.1. Project Overview

The Chongqing Nanjimen track bridge [29] is the world's largest span special track cable-stayed bridge; its structure is a five-span high–low tower double-cable plane semi-floating system with a span arrangement of 34.5 m + 180.5 m + 480 m + 215.5 m + 94.5 m. The main beams are in the form of mixed steel beams, and the bridge tower is in the form of a gate tower, of which the total height of the low tower is 158m and the total height of the high tower is 227 m. The cable is made of a Φ7.0 mm galvanized high-strength low-relaxation parallel-steel HDPE-sheath-finished cable; its tensile strength is not less than 1770 MPa, the tensile elastic modulus is not less than 195,000 Mpa. The cable is made of a 5% zinc–aluminum mixed rare earth alloy coating. The wire is arranged in a compact, concentric twist, and the outer layer of the wire is twisted at an angle of 3.5° to the left. The outer layer of the cable consists of a high-density polyethylene sheath and incorporates a weather-resistant double helix coil design. A total of 27 pairs of permanent cables are installed on the side of a high tower and 16 pairs of cable-stayed cables are installed on the side of a low tower (for the overall layout of the Chongqing Nanjimen track bridge, see Supplementary Document Figure S1).

2.2.2. COMSOL Segment Model

- Material parameters of the steel–concrete composite beam model.

The steel–concrete composite beam (SCCB) is mainly composed of steel and concrete materials. This research mainly considers the influence of solar radiation on structural materials and temperature fields. Materials are set according to Equations (2)–(4). Material

parameters include thermal conductivity, specific heat capacity, absorptivity, emissivity, etc. The specific performance parameters are shown in Table 1. The short-wave absorptivity mainly considers solar radiation and the long-wave absorptivity mainly considers environmental radiation.

Table 1. Thermal performance parameters of materials.

Material Property	Steel (Q345qD)	Concrete (C60)
Density (kg/m^3)	7850.0	2500.0
Specific heat capacity (j/kg·°C)	460.0	960.0
Coefficient of heat conduction (w/m·°C)	58.2	2.94
Coefficient of thermal expansion (1/°C)	12×10^{-6}	10×10^{-6}
Shortwave absorption rate	0.3	0.65
Long wave absorption rate	0.8	0.85

- The model setting of COMSOL.

1. Climate parameters.

Under the action of solar radiation, air temperature usually changes according to a certain law, and the sine and cosine function is generally used to describe the temperature change in actual calculation. According to the research in the literature [30,31], the atmospheric temperature is expressed by the following cosine function:

$$T_a(t) = T_1 + \frac{T_2}{2}\cos\frac{\pi(t - t_m)}{12}, 0 \le t \le 24 \quad (7)$$

where T_1 and T_2 represents the daily mean value and daily fluctuation value of air temperature in the corresponding period. In this document, the values are 32.0 °C and 12.0 °C, respectively. t indicates the time of day, h. t_m is the time when the highest temperature appears, which in this paper is 15:00.

2. Solar radiation settings.

The solar radiation interface of COMSOL 6.2 can automatically calculate the declination angle, solar hour angle, solar altitude angle, azimuth angle, and ray incidence angle based on the longitude, latitude, and time zone of the target point, thereby applying solar radiation loads. The Chongqing Nanjimen track bridge is located in Chongqing, China, latitude 29.55° N, longitude 106.59° E. The time zone is East 8 zone (UTC/GMT+08:00). The solar irradiance is set at 1000 W/m^2, and the horizontal scattering irradiance in the clear sky at noon is 150 W/m^2.

- Establishment of a mixed steel segment model.

COMSOL6.2 was used to establish the section model of the main beam of the Chongqing Nanjimen track bridge, simulate the temperature field change under solar radiation, select the section with the thickness of 260 mm concrete slab in the span, construct the superimposed beam model with a length of 7 m through Soildwork 2023, and introduce it into COMSOL6.2 to form a solid and automatically build a consortium. The model consists of 3 domains and 81 boundaries. Using physical field control to refine the grid, the complete grid contains 54,559 domain units, 35,672 boundary units, and 2236 edge units, and the number of degrees of freedom to solve is 145,148 (including 75,997 internal degrees of freedom), as shown in Figure 1. To deal with complex problems more effectively, concentrate research resources and ensure the practicability of the model, the following assumptions are made in this paper: (1) The model has good contact with air, and air is assumed to be a uniform medium. (2) The materials used in the model are assumed to be homogeneous materials, and there is no difference in the thermal performance of a single material. (3) The solar radiation uses COMSOL6.2 with solar radiation interface, convection heat transfer

and radiation heat transfer using the third type of boundary conditions, air heat transfer coefficient of 10 W/(m^2·K). (4) The initial moment of the model is 0 o'clock, and the initial temperature is the lowest temperature in a day (the ambient temperature before sunrise is used as the initial value of the bridge temperature field calculation): 27.0 °C. (5) Since the bridge runs north–south, it is assumed that the temperature field in the longitudinal direction of the bridge does not change, and the end face of the beam section is an insulating surface. (6) The shading effect and influence of bridge towers, cable-stayed cables, bridge deck pavements and track equipment are not considered. The segment model diagram is shown in Figure 1.

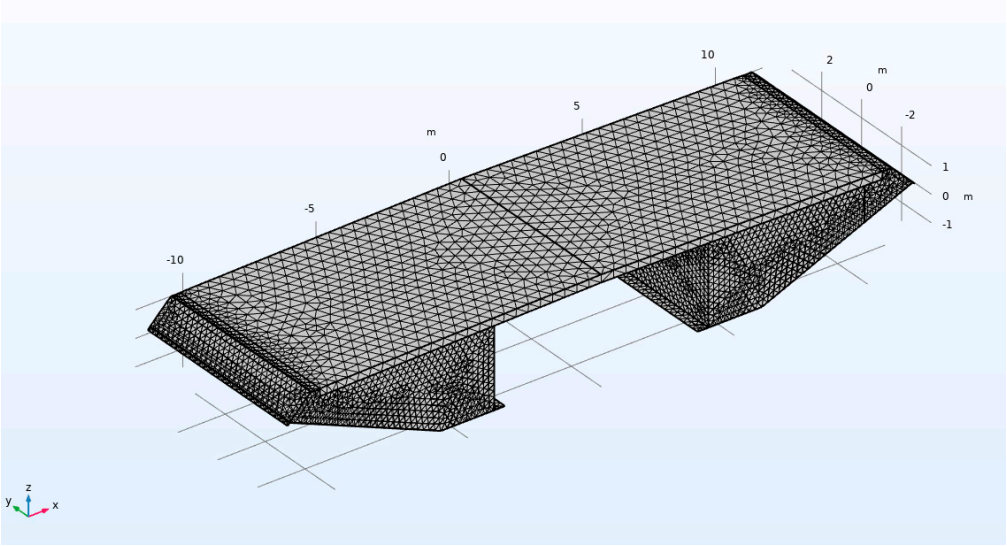

Figure 1. Grid model diagram of the main girder section of Chongqing Nanjimen track bridge.

- Verification of mixed steel segment model.

To verify the accuracy of the steel mixture segment model, 24 h of a certain day (25 January 2023) was randomly selected to compare the finite element predicted temperature obtained by COMSOL simulation with the actual temperature, and the mean absolute error (*MAE*) [25] was used to evaluate the consistency between the predicted temperature and the recorded temperature. The mean absolute error is the sum of the absolute difference between the predicted and recorded temperatures for all time steps divided by the number of individuals, calculated as follows:

$$MAE = \frac{1}{N}\sum i = \frac{1}{N}\sum |y_i - y_j| \quad (8)$$

where y_i is the simulated temperature and y_j is the measured temperature.

To eliminate the influence of initial temperature on the temperature field of the steel-hybrid beam and improve the accuracy of the calculation [32], based on the COMSOL segment model, a 6-day simulation with a step length of 0.5 h was carried out, and the data of the sixth day was used for verification. The results are shown in Figure 2. The mean absolute error (MAE) between simulated and measured temperatures on the east and west sides was calculated by Formula (8). The smaller the MAE value, the higher the degree of fit, and the calculated results were 0.10 °C and 0.06 °C, respectively, indicating that the model adopted met the requirements of simulation calculation.

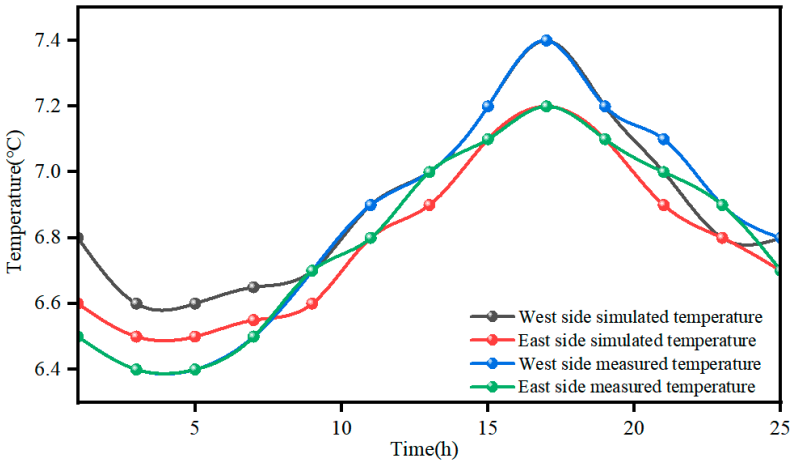

Figure 2. Comparison of simulated temperature and measured temperature in 24 h on 25 January 2023.

2.2.3. Midas/Civil Bridge Model

The MIDAS/Civil 2023 was used to establish the full bridge model of the Chongqing Nanjimen track bridge, and the numerical simulation of the temperature difference and temperature gradient of the system was carried out. There were 1085 nodes and 1504 elements of the whole bridge, among which cable elements were used for the stay cable, beam elements were used for the main tower, bridge panel, and main beam, and composite beam simulation was carried out for the bridge panel and main beam by the double-element method. The cable anchorage uses a rigid connection, the base of the main tower adopts general support with a solid connection, and the boundary constraint between the main beam, main tower, and bridge pier are elastic connections. The number of iterations is set to 20 in the master data, and the convergence error is 0.001. In the construction phase, nonlinear analysis and time-varying effect are considered, tangential assembly is considered for the main beam, and the cable force of the cable is controlled by external force, as shown in Figure 3.

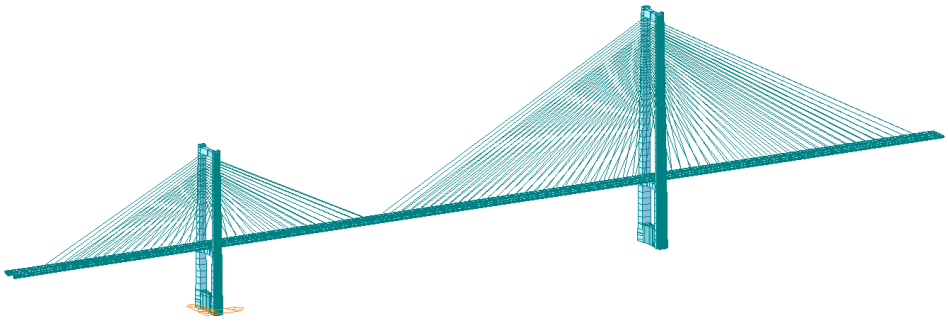

(**a**)

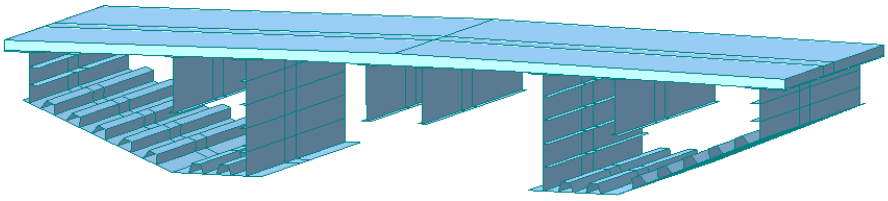

(**b**)

Figure 3. *Cont.*

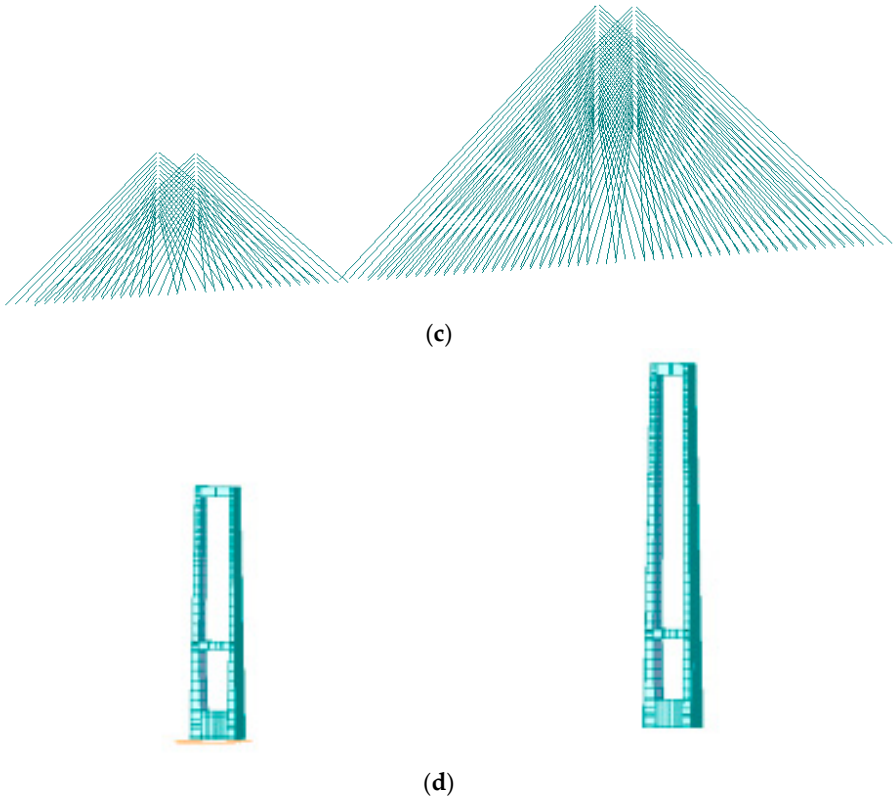

(**c**)

(**d**)

Figure 3. The overall finite element model of the Chongqing Nanjimen track bridge. (**a**) Discrete diagram of the overall finite element model. (**b**) Finite element model of the main girder section. (**c**) Finite element model of the stay cable section. (**d**) Finite element model of the main tower section.

3. Analysis of the Temperature Field of Steel–Concrete Superimposed Beam (SCCB)

3.1. Temperature Distribution in the Cross-Section

To eliminate the impact of the structure's initial temperature on the temperature field of the steel-hybrid beam, this paper eliminates the influence of the initial temperature by extending the calculation period according to the research in the literature [32]. When the temperature changes and solar radiation are the same, the simulation results of day 6 are analyzed. At the same time, to reduce the influence of longitudinal boundary conditions on the simulation results, the middle section of the segment was used to sample the results [33]. The extraction position diagram is shown in Figure 4, and the temperature field distribution results are shown in Figure 5 (in Figure 4a, positive X, Y, and Z directions represent due east, due north and the sky direction, respectively, and the sun incident direction is rising in the east and setting in the west).

As can be seen from Figure 5, from 1:00 to 5:00, after the loss of the external heat source (solar radiation), the overall temperature gradually drops, and the maximum temperature drops from 46.0 °C to 44.8 °C. Because the thermal conductivity of concrete is lower than that of steel structure, the temperature drop rate inside the concrete slab is slower than that of the steel beam, so the temperature of the concrete slab is always higher than that inside the box beam. In addition, because the air inside the box beam is not circulated, although the external ambient temperature is reduced, the steel box still retains a certain amount of heat, forming an obvious temperature gradient. The lowest temperature throughout the day appears at 5:00 and the lowest temperature is 34.0 °C, located at the bottom of the steel beam. Meanwhile, the maximum temperature inside the structure is 44.8 °C, located at the concrete slab above the steel beam, and there is a temperature gradient of 10.8 °C inside the box beam. Between 5:00 and 15:00, as the sun rises, the overall temperature gradually rises, with the maximum temperature rising from 44.8 °C to 60.3 °C. The highest temperature occurs at 15:00, reaching 60.3 °C, which is located on the top of the concrete slab above the

steel beam. At this time, the lowest internal temperature of the structure is 43.0 °C, which appears in the suspended position of the concrete slab. Between 15:00 and 20:00, the sun gradually drops, the temperature gradually decreases, and the maximum temperature of the main beam drops from 60.3 °C to 47.0 °C.

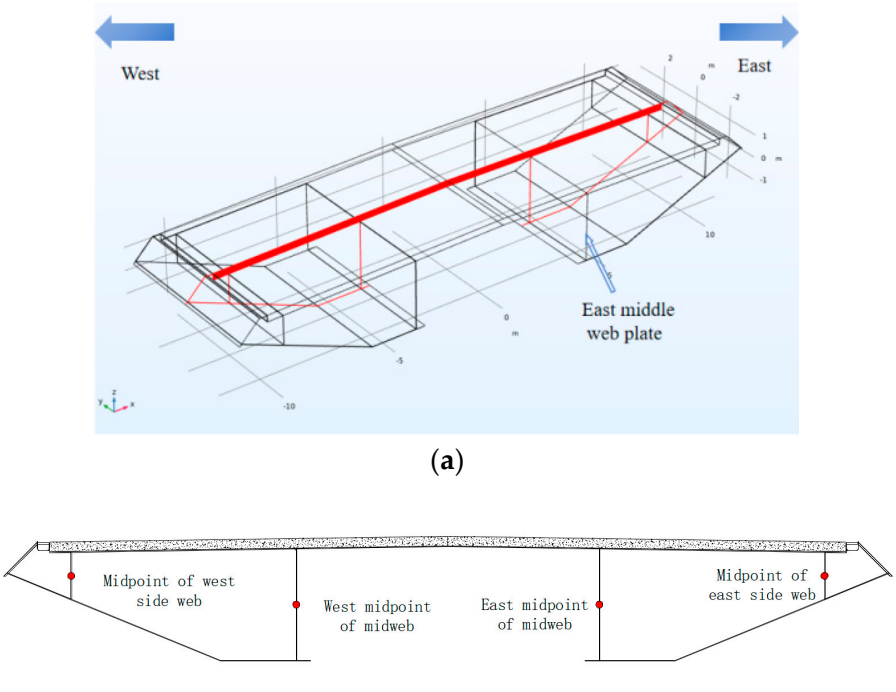

(**a**)

(**b**)

Figure 4. Schematic diagram of result extraction position. (**a**) Diurnal temperature field cloud image and vertical temperature extraction position. (**b**) Diagram of transverse temperature extraction point of steel beam.

It can be seen that under the same ambient temperature change, the temperature field distribution of the steel-hybrid beam presents obvious nonlinear characteristics, the daily temperature difference is as high as 26.0 °C, and the internal temperature gradient is obvious. Therefore, in the process of construction and design, special attention should be paid to the influence of temperature. During the operation phase, temperature changes need to be continuously monitored to ensure the normal operation of the bridge.

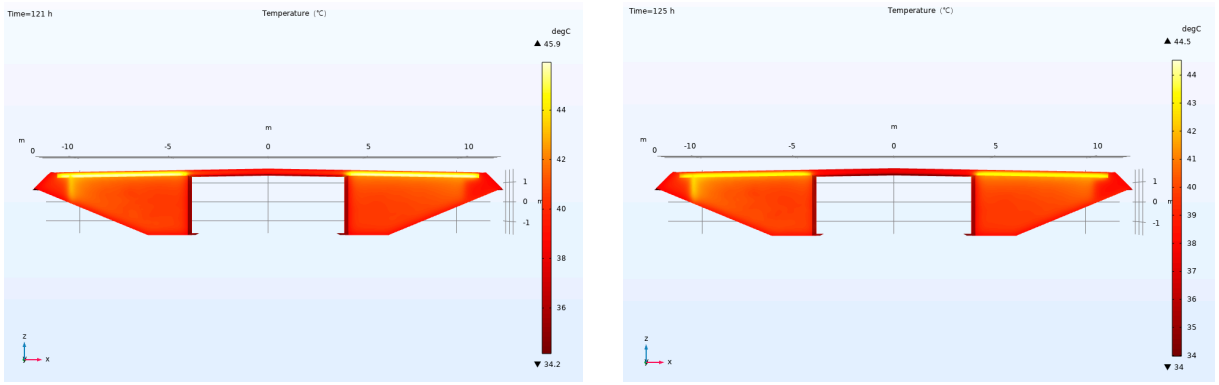

(**a**) (**b**)

Figure 5. *Cont.*

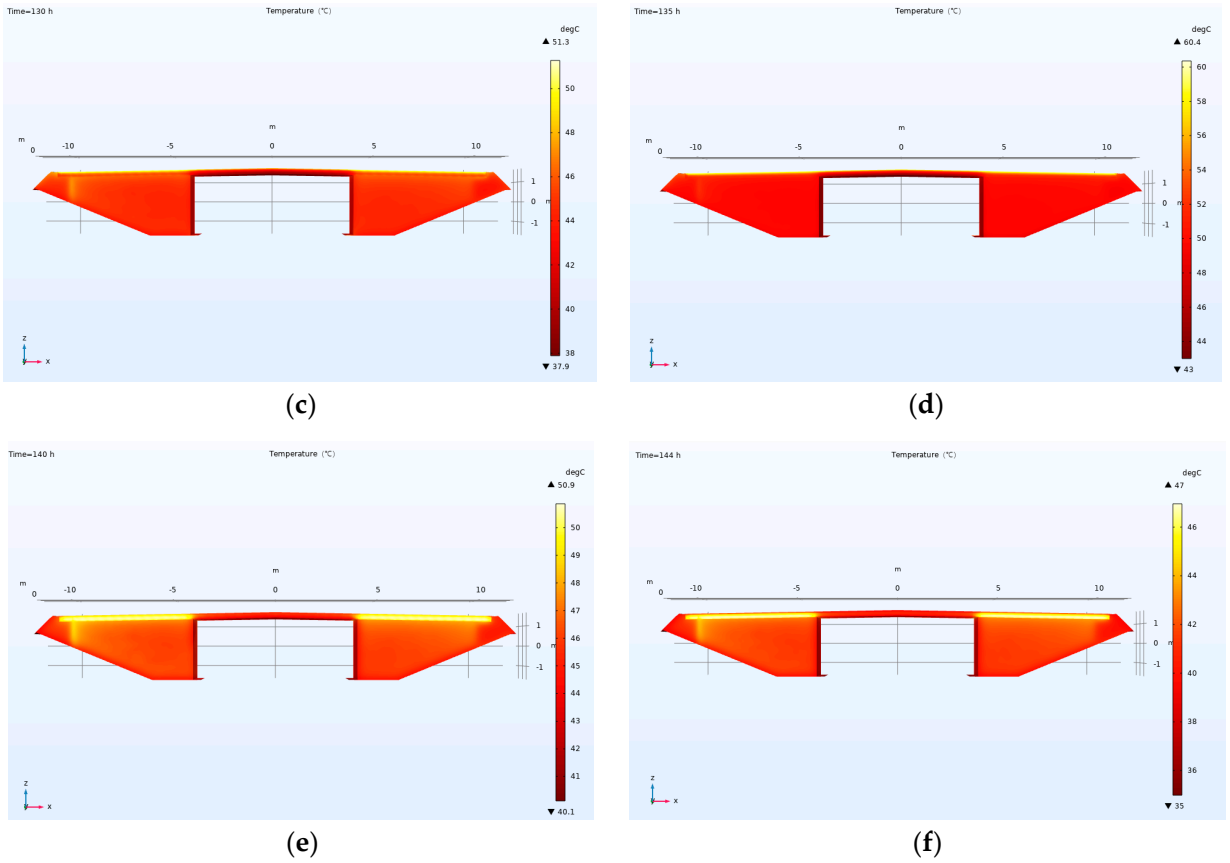

(**c**) (**d**)

(**e**) (**f**)

Figure 5. Distribution cloud of daily temperature field of steel–concrete composite beam. (**a**) 1:00. (**b**) 5:00. (**c**) 10:00. (**d**) 15:00. (**e**) 20:00. (**f**) 24:00.

3.2. Transverse and Vertical Temperature Distribution Analysis

3.2.1. Vertical Temperature Gradient

Taking the vertical temperature distribution in the center of the eastern mid-web as the research object, the 24 h temperature gradient change in the steel-hybrid beam under sunshine is analyzed, as shown in Figures 6–9.

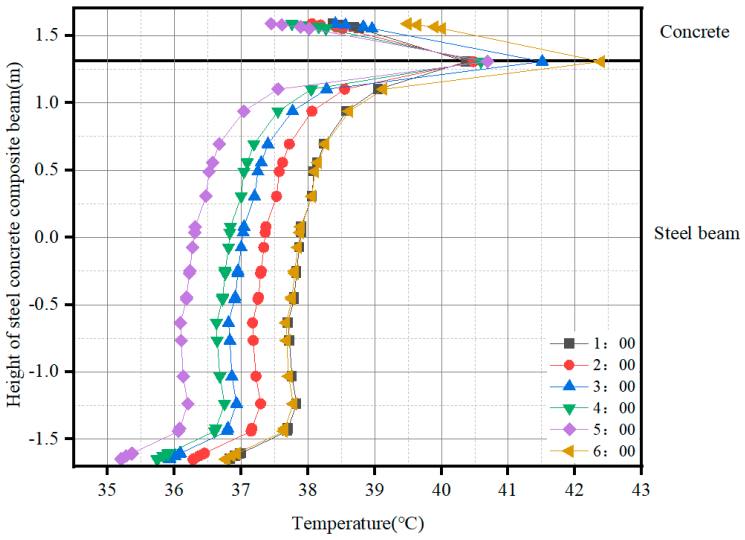

Figure 6. Vertical temperature distribution of the east side web from 1:00 to 6:00.

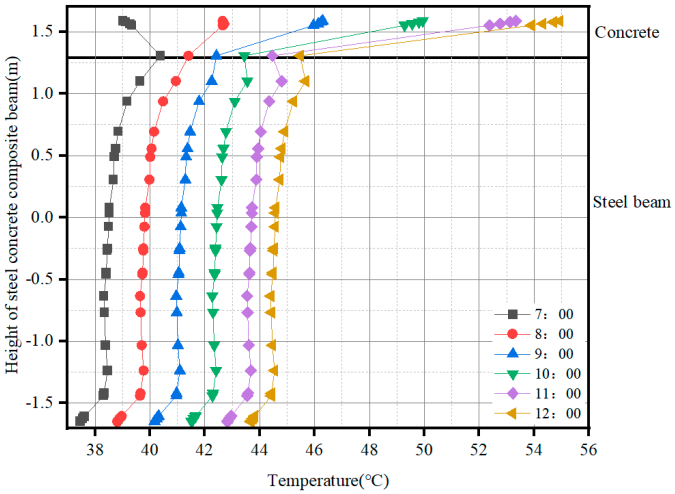

Figure 7. Vertical temperature distribution of the east side web from 7:00 to 12:00.

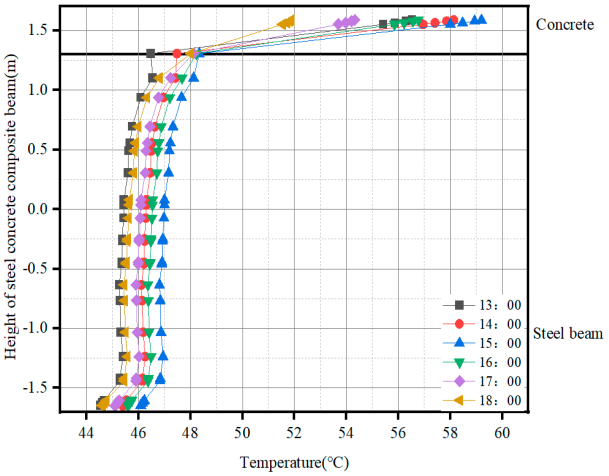

Figure 8. Vertical temperature distribution of the east side web from 13:00 to 18:00.

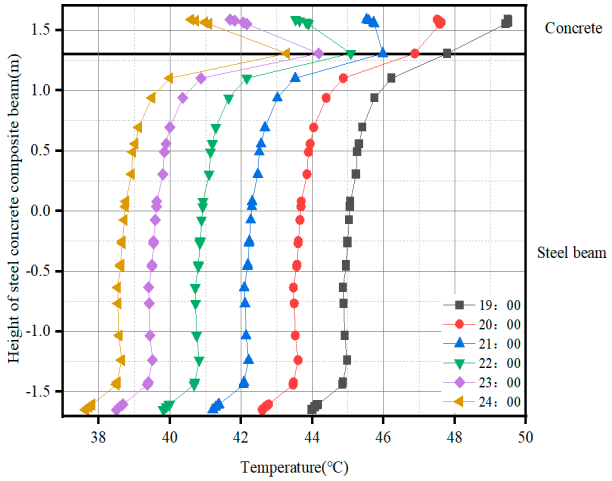

Figure 9. Vertical temperature distribution of the east side web from 19:00 to 24:00.

According to Figures 6 and 7, during the period of 1:00 to 5:00, in the absence of external radiation sources, the steel beam and concrete slab continue to radiate outward and dissipate heat, and the temperature gradually decreases, reaching the daily minimum

temperature at 5:00 am. The temperature distribution inside the concrete slab presents an inverse "C" curve. Because the air in the steel beam has a thermal insulation effect, the temperature of the steel beam near the concrete slab is higher and has a certain temperature gradient. During this period, the temperature difference between the upper edge and the lower edge of the steel beam reached a maximum of 5.6 °C. However, the internal temperature of the steel beam is higher than the ambient temperature, and the bottom of the steel beam continues to dissipate heat, so there is a temperature gradient of 1.0 °C from the bottom of the steel beam. From 7:00 to 12:00, with the rise of the sun, the ambient temperature rises. Under the action of solar radiation, the temperature of the upper edge of the concrete slab increases rapidly, and the temperature of the lower edge of the concrete slab and the steel beam also increases slowly. The temperature difference between the upper and lower edges of the concrete slab gradually increases, and the temperature difference reaches a maximum of 9.0 °C at 12:00. The temperature inside the steel beam gradually increases, and the temperature gradient at the bottom of the steel beam decreases to 0.6 °C.

As can be seen from Figures 8 and 9, the temperature gradually rises during 13:00–15:00. The temperature drops gradually from 15:00 to 18:00. The maximum temperature of the concrete slab and steel beam appeared at 15:00, which were 59.2 °C and 48.1 °C, respectively. At this time, the temperature difference between the upper and lower edges of the concrete slab reaches a maximum of 11.1 °C, but the temperature difference between the upper and lower edges of the steel beam is only 2.2 °C. With the decrease in ambient temperature and solar radiation intensity, the temperature of the upper edge of the concrete slab gradually decreases. During 14:00~18:00, the overall temperature change range of the lower edge of the concrete slab and the internal temperature of the steel beam is less than 1.0 °C, and the temperature gradient at the bottom of the steel beam is only 0.6 °C. After 19:00, as the external radiation source is lost, the ambient temperature gradually decreases, the temperature of the upper edge of the concrete slab and the steel beam begins to decrease, the temperature of the lower edge of the concrete slab slowly decreases, and the temperature inside the concrete slab gradually forms an inverse "C" curve. The temperature gradient at the bottom of the steel beam increased to 0.9 °C, and the temperature difference between the upper and lower edges of the concrete slab gradually increased, reaching 3.3 °C at 24:00.

In summary, the temperature gradient of steel–concrete composite beams is significantly affected by the external environment and radiation and changes with time, and its unique heat conduction characteristics significantly affect the overall temperature distribution of the structure. Under the condition of no radiation, the heat exchange effect between the steel beam and the concrete slab is remarkable. The significant temperature difference between the upper and lower edges of the concrete slab will have a potential impact on the tensile and compressive performance of the concrete, but the steel beam has a good thermal insulation property inside, which can delay the overall temperature change to a certain extent, proving that the steel-hybrid beam has good adaptability to temperature, especially in the environment with a large temperature difference, and can effectively reduce the impact of temperature stress on the structure.

3.2.2. Horizontal Temperature Distribution

- Transverse temperature distribution of concrete slab.

The transverse temperature change in the beam section does not cause vertical additional bending moment, but it leads to significant temperature self-stress. Therefore, the transverse temperature changes in the upper, middle, and lower edges of the concrete slab are studied in detail in this paper. Figures 10–12 show the transverse temperature change in the upper, middle, and lower edges of the concrete slab in one day, where the negative scale area on the horizontal coordinate represents the west side and the positive scale area represents the east side.

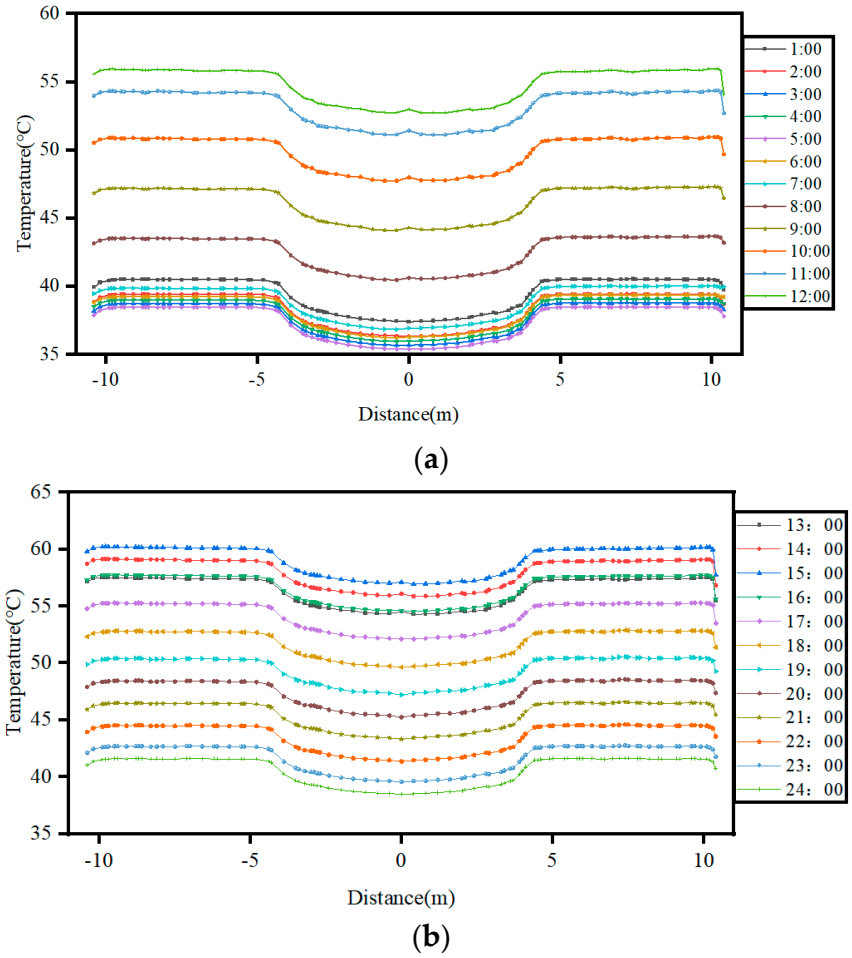

Figure 10. Transverse temperature change at the upper edge of the concrete. (**a**) Change between 1:00 and 12:00. (**b**) Change between 12:00 and 24:00.

It can be seen in Figure 10 that the overall transverse temperature of the upper edge of the concrete slab changes gently, but there is a certain temperature difference between the east and west borders. Due to the insulation effect of the steel box girder, the temperature of the concrete slab above the steel beam is always higher than the middle position, and the maximum temperature difference between the two reaches 3.2 °C. The upper edge of the concrete slab reaches the lowest temperature of 35.4 °C at 5:00, the maximum temperature of 60.2 °C at 15:00, and the daily temperature difference in the upper edge of the concrete slab is 24.8 °C.

As seen in Figure 11, the overall trend of transverse temperature distribution in the middle of the concrete slab is the same as that on the upper slab, except for the difference in value. The temperature in the middle of the concrete slab between the steel boxes is always lower than the temperature of the concrete slab above the steel box, and the temperature difference is about 5.3 °C. The upper edge of the concrete slab reaches the lowest temperature of 35.5 °C at 5:00, the maximum temperature of 53.9 °C at 15:00, and the daily temperature difference in the upper edge of the concrete slab is 18.4 °C.

It can be seen from Figure 12 that the temperature variation law of the lower edge of the concrete slab is similar to that of the upper and middle of the concrete slab, except in numerical value. The temperature difference between the lower edge of the concrete slab between the steel box and the lower edge of the concrete slab above the steel box reaches a maximum of 7.4 °C at 19:00. The minimum temperature of the whole day is 35.7 °C, the maximum temperature is 52.3 °C, and the daily temperature difference at the lower edge of the concrete slab is 16.6 °C.

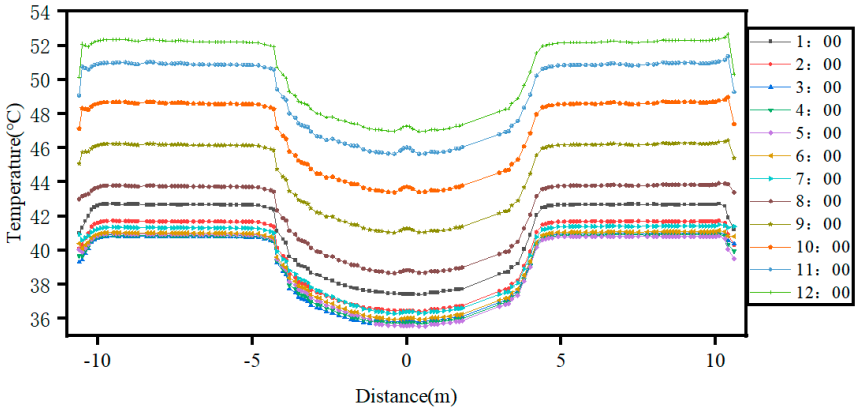

(**a**)

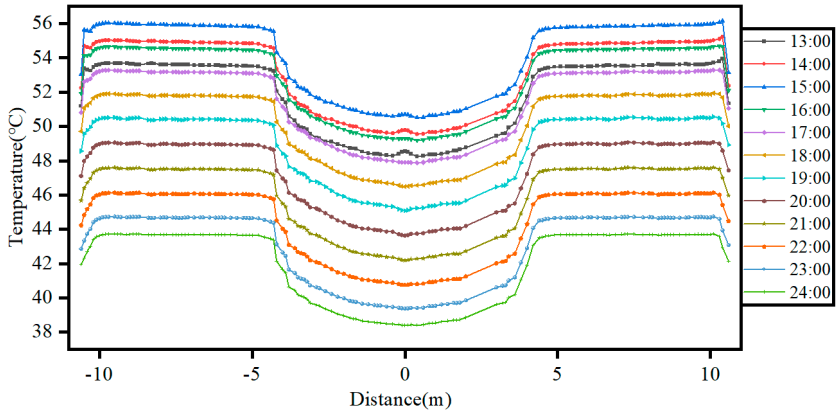

(**b**)

Figure 11. Transverse temperature change at the middle edge of the concrete. (**a**) Change between 1:00 and 12:00. (**b**) Change between 12:00 and 24:00.

- Steel beam web temperature distribution.

According to the positions shown in Figure 6, the temperature data of the midpoint of the east–west side web, the midpoint of the east side web and the midpoint of the COMSOL model were extracted, the temperature data inside the steel beam were analyzed, and the results were shown in Figure 13.

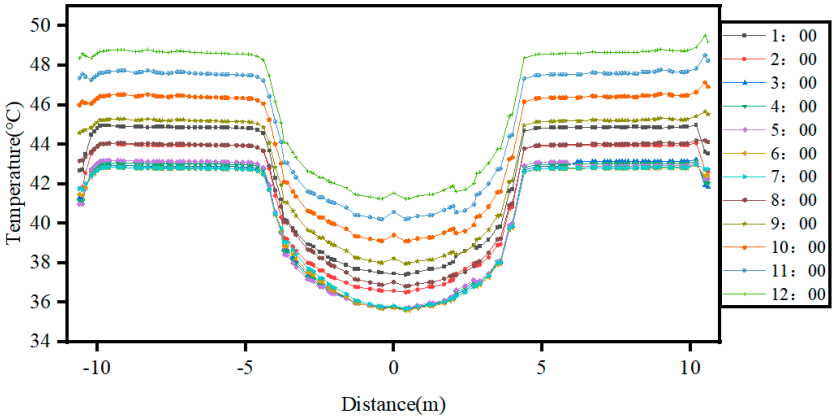

(**a**)

Figure 12. *Cont*.

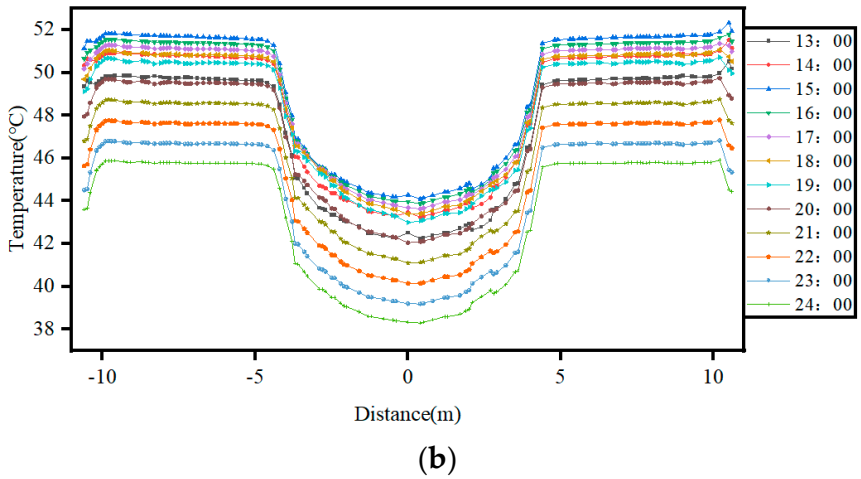

(**b**)

Figure 12. Transverse temperature change at the lower edge of the concrete. (**a**) Change between 1:00 and 12:00. (**b**) Change between 12:00 and 24:00.

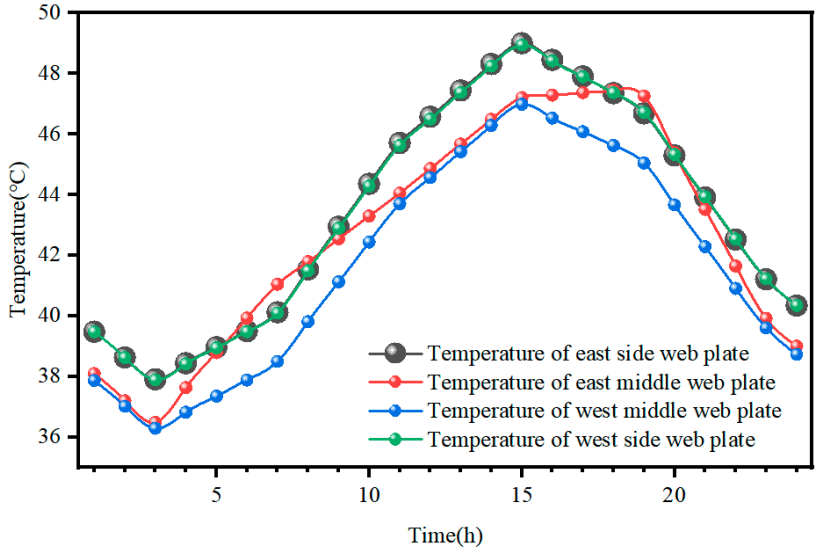

Figure 13. Temperature change in steel beam web in one day.

It can be seen from Figure 13 that the temperature at the midpoint of the east and west side webs and the side web on a 24 h day shows the same trend in the form of cosine function. The temperature at the midpoint of the mid-web on the east and west sides varies slightly from day to day, but the overall trend is the same. Both sides of the midpoint of the side webs are in a closed-air environment, the air flow is small, the steel box girder has a certain insulation effect, and the temperature of the east and west side webs is basically the same. The east–west side of the web presents a certain fluctuation, which is because the side of the web is in contact with the environment, and the insulation effect is weak. From 5:00 to 15:00, the temperature of the eastern mid-web gradually rises due to the rising sun, reaching the maximum at 15:00; as the sun gradually began to fall, the temperature of the western mid-web was gradually higher than that of the eastern mid-web, showing obvious time-domain characteristics.

In summary, the transverse temperature distribution of steel–concrete composite beams shows obvious temporal and spatial characteristics. Under the action of solar radiation, because the heat of the concrete slab near the box girder is more likely to be affected by the insulation of the air inside the box girder, the transverse temperature distribution of the upper, middle and lower edges of the concrete slab has a significant temperature gradient, and the daily transverse temperature gradient of the upper, middle

and lower edges of the concrete slab is 3.2 °C, 5.3 °C and 7.4 °C, respectively. The closer the concrete slab is to the steel beam, the greater the transverse temperature gradient is. Due to the unique structure and insulation characteristics of the steel beam, the temperature changes in the east and west side web and the middle web are basically the same. The transverse temperature distribution inside the steel beam is uniform, indicating that the design of the steel beam can effectively reduce the influence of external temperature changes on the internal structure and improve the overall temperature stability. Under the environmental conditions of large temperature fluctuations, this structural form can improve and maintain the strength and durability of the structure through the form of steel mixing.

4. Influence of System Temperature Difference and Temperature Gradient on Vertical Deformation of the Whole Bridge

4.1. Value of System Temperature Difference and Temperature Gradient

The Chongqing Nanjimen track bridge will be closed on 25 January 2022, with a closing temperature of 7–11 °C. According to the data of the Chongqing Meteorological Bureau, the annual average temperature of the bridge site is 18.3 °C, and the extreme maximum temperature is 43 °C. The date of occurrence is 15 August 2006. The daily minimum temperature was −1.8 °C on 15 December 1975. According to Equations (5) and (6), the temperature load values are obtained as follows. (1) Temperature difference in the system: the overall temperature rise is considered as 43.0 °C − 7.0 °C = 36.0 °C, and the overall temperature drop is considered as 11.0 °C − (−1.8 °C) = 12.8 °C ≈ 13. (2) Temperature gradient of the main beam: the positive temperature difference in the beam temperature gradient is taken as the temperature difference between the concrete slab and the steel beam +10.0 °C, and the negative temperature difference in the beam temperature gradient is taken as the temperature difference between the concrete slab and the steel beam −10.0 °C.

4.2. Vertical Deformation of Main Beam Under Temperature Action

4.2.1. Vertical Deformation of Main Beam Under the Action of Temperature Difference in System

Midas Civil 2023 was used to simulate the vertical deformation of the main beam under the effect of the temperature difference in the system (overall temperature rise of 36.0 °C and overall temperature drop of 13.0 °C), and the results are shown in Figure 14. Among them, the vertical downward movement of the vertical coordinate is positive, the vertical upward movement is negative, and the horizontal coordinate 0 point represents the position of station A0, the same as below.

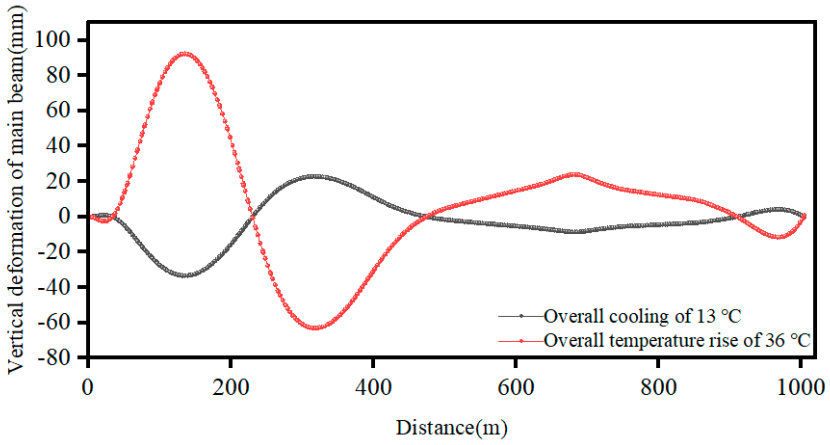

Figure 14. Vertical deformation of main beam under temperature difference in system.

As can be seen from Figure 14, under the action of overall temperature rise, the main beams on both sides of the high and low towers are deformed vertically upward,

while those in the middle of the span are deformed vertically downward. The maximum deformation of the main beam on the side of the high tower is 23.9 mm, 682.1 m away from station No. A0. The maximum deformation of the main beam on the side of the low tower is 92.3 mm, 135.6 m away from station A0. The maximum vertical downward deformation in the span is −63.1 mm, 318.1 m away from station A0, near the side of the low tower. Under the effect of overall cooling, the deformation trend of the main beam is opposite, and the maximum deformation of the main beam on the side of the high tower is −8.6 mm, 682.1 m away from station No. A0. The maximum deformation of the main beam on the side of the low tower is −33.3 mm, 135.6 m away from station A0. The maximum vertical downward deformation in the span is 22.8 mm, 318.1 m away from station A0, near the side of the low tower. Affected by the temperature difference in the system, the maximum deformation of the side span of the low tower is much higher than that of the side of the high tower.

Because the Chongqing Nanjimen track bridge is a semi-floating system, the expansion and deformation of the main beam are limited, and the vertical deformation of the main beam mainly depends on the deformation of the cable and tower under the temperature difference in the system. When the overall temperature rises, the structure of the bridge tower expands and extends, and the extension of the flange on the main beam affects the angle of the cable. In addition, the cable expands and expands under the action of temperature, and the tension increases. The further the cable is from the main tower, the greater the expansion amount, resulting in the rise of the main beam and the opposite of the cooling of the system. Under the action of system temperature difference, the overall deformation value of the bridge fluctuates greatly, which has an adverse effect on the alignment of the bridge and has a great influence on the ride comfort and comfort of the train. Therefore, in the daily management and maintenance of the track bridge, more attention should be paid to the monitoring of the temperature and stress of the main beam on both sides of the main tower to ensure the safe, stable and comfortable operation of the bridge.

4.2.2. Vertical Deformation of Main Beam Under the Action of Temperature Gradient

Midas Civil 2023 was used to simulate the vertical deformation of the main beam under positive and negative temperature differences, and the vertical deformation of the main beam under the temperature gradient load of ±10.0 °C temperature difference between the concrete slab and the steel box beam was obtained, as shown in Figure 15.

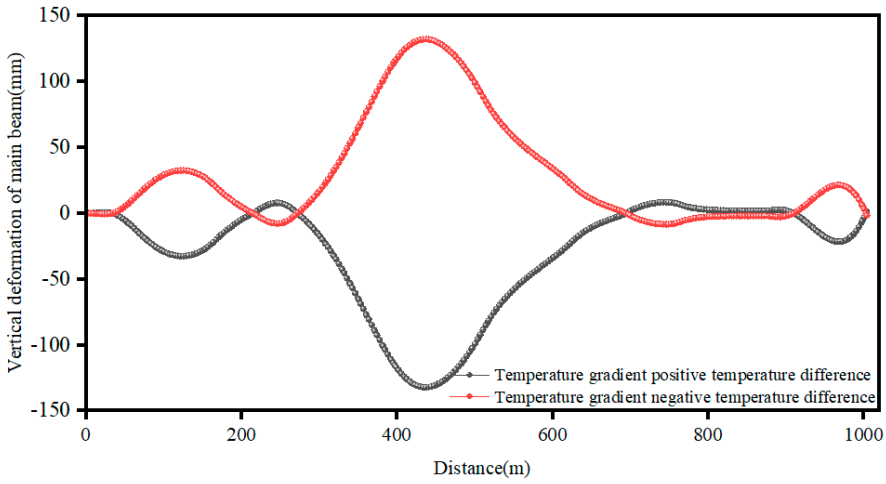

Figure 15. Vertical deformation of main beam under the action of temperature gradient.

As observed from Figure 15, under the effect of positive temperature difference in temperature gradient, the overall deformation trend of the main beam is vertical upward, and its maximum value appears near the mid-span, which is 132.1 mm at 437.1 m away

from station No. A0. The deformation value of the main beam at the low and high tower sides changes little, and the whole deformation shows vertical downward. Among them, the minimum deformation of the low tower side is −7.8 mm, which is 245.3 m away from station No. A0. The minimum deformation value on the side of the high tower is −8.4 mm, which occurs at 745.6 m away from station A0. Under the effect of positive temperature difference in temperature gradient, the upper flange of the main beam extends, resulting in an upward trend, but the longitudinal deformation of the main beam causes the inclination of the stay cable to decrease, and the length of the stay cable remains unchanged. Under the vertical constraint of the auxiliary pier, the two main towers tilt to the side span and the middle span main beam is twisted. The vertical deflection of the main beam caused by a negative temperature difference is opposite to that caused by a positive temperature difference.

5. Structure Measured Temperature and Deformation Analysis

5.1. Structural Temperature and Deformation System

The temperature and deformation monitoring system of the Chongqing Nanjimen track bridge structure adopts a temperature and humidity sensor to measure the ambient temperature change in the bridge and adopts a GNSS deformation system to monitor the deformation of the main beam, and obtains the transverse, longitudinal and vertical spatial deformation data of the main beam, which provide an important basis for the state assessment of the bridge structure. The ambient temperature measuring point and the three-way deformation monitoring point of the main beam are arranged at the closing section of the main span of the main bridge (the Chongqing Nanjimen track bridge structural temperature and deformation system overview see Supplementary Document Figure S2).

5.2. Temperature Field Test Data and Analysis

To fully obtain the temperature field of the structure under the condition of periodic climate change, the temperature observation time is set to one year, that is, January to December 2023. For bridge structures subjected to solar radiation and atmospheric temperature changes, the most unfavorable vertical positive temperature difference can be generated in summer when solar radiation is intense, and the most unfavorable vertical negative temperature difference can be generated under the effect of sudden atmospheric cooling in winter [16]. According to the annual temperature test data, the temperature measurement point data from 00:00 to 23:29 on 17 August 2023 were selected as the summer analysis data. The maximum ambient temperature inside and outside the box girder was 37.9 °C and 36.4 °C, respectively. The temperature measurement point data from 00:00 to 23:29 on 18 January 2023 is selected as the winter analysis data. The minimum ambient temperature inside and outside the box girder is 4 °C and 6.3 °C, respectively. Using the measuring point of the concrete bridge panel in the middle section of the main span, the obtained data are shown in Figure 16.

As can be seen from Figure 16, during the coldest month in winter and the hottest month in summer, the ambient temperature presents an obvious cosine function form, and the maximum temperature difference is 2.1 °C and 7.5 °C, respectively. During the period from 0:00 to 5:00, the temperature gradually decreases, while at 6:00 to 15:00 the temperature gradually rises and reaches the maximum at 15:00. After 15:00, as the sun gradually goes down, the temperature begins to slowly decrease, eventually reaching a new thermal equilibrium. Due to the limited temperature measurement points in the box, all located at the bottom of the steel box girder, the overall temperature changes gently, and the maximum value appears at around 15:00 in the afternoon, which is consistent with the results of the temperature field simulation.

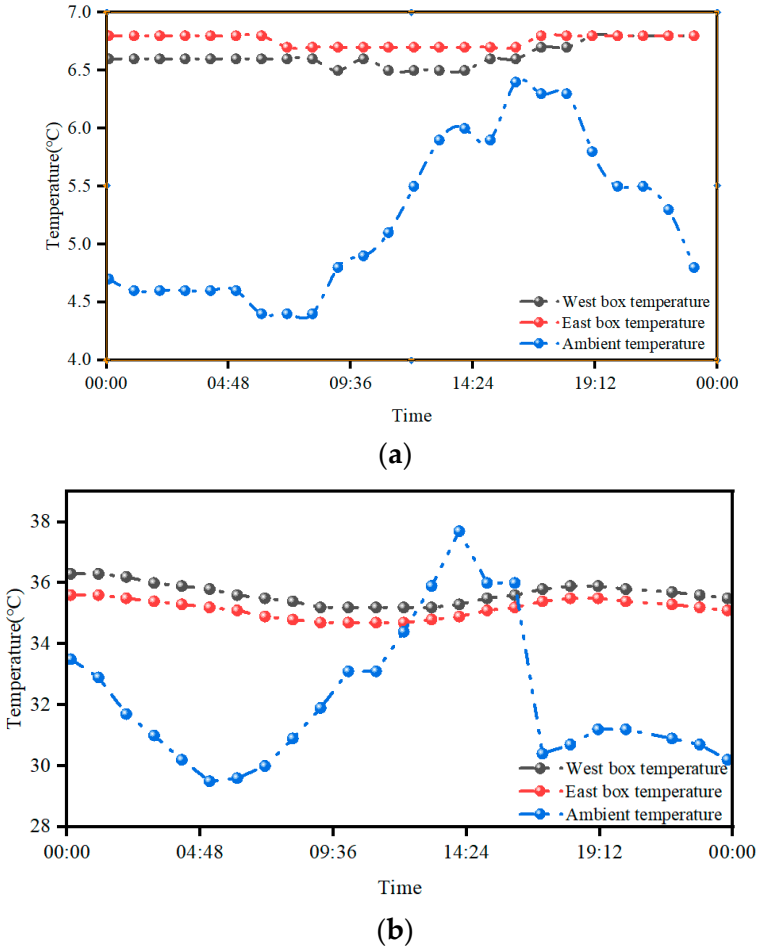

Figure 16. Ambient temperature and east and west box temperature. (**a**) Ambient temperature and east and west box temperature on January 18. (**b**) Ambient temperature and east and west box temperature on 18 January 2023.

5.3. Measured Deformation of Main Beam

Based on the obvious difference in signal frequency and amplitude between the train load effect and temperature load effect, the adaptive filtering method proposed in the literature [34] is adopted in this paper to extract the deformation of the bridge under the action of temperature in the structural response data, as shown in Figure 17.

As can be seen from Figure 17, under the influence of temperature change, the deformation trend of the main beam in winter and summer is similar, but the specific values are different, and the deformation on the east side is greater than that on the west side. The high temperature in summer causes thermal expansion of the material, resulting in the increase in the transverse deformation of the main beam, and the maximum transverse deformation is 36.4 mm, which appears around 16:00. The shrinkage of the material caused by low temperature in winter causes the lateral deformation to fluctuate around the reference point. In the hottest summer, the vertical deformation of the main beam continues to increase, reaching a maximum value of −274.4 mm at about 15:00. In the coldest winter, the vertical deformation of the main beam reaches a maximum value of −203.6 mm at about 18:00. Due to the lag effect of temperature, the time when the maximum deflection appears is different from that in summer, and the value is smaller. Under the action of temperature difference and temperature gradient of the system, the deformation of the main beam with the same section is compared. It is found that the deformation of the main beam with section of the main beam span is −29.7 mm when the temperature rises. Under the positive temperature difference, the deformation of the main beam of section of the main beam span is −119.2 mm, while the vertical deformation of the main beam is −274.4 mm at 15:00.

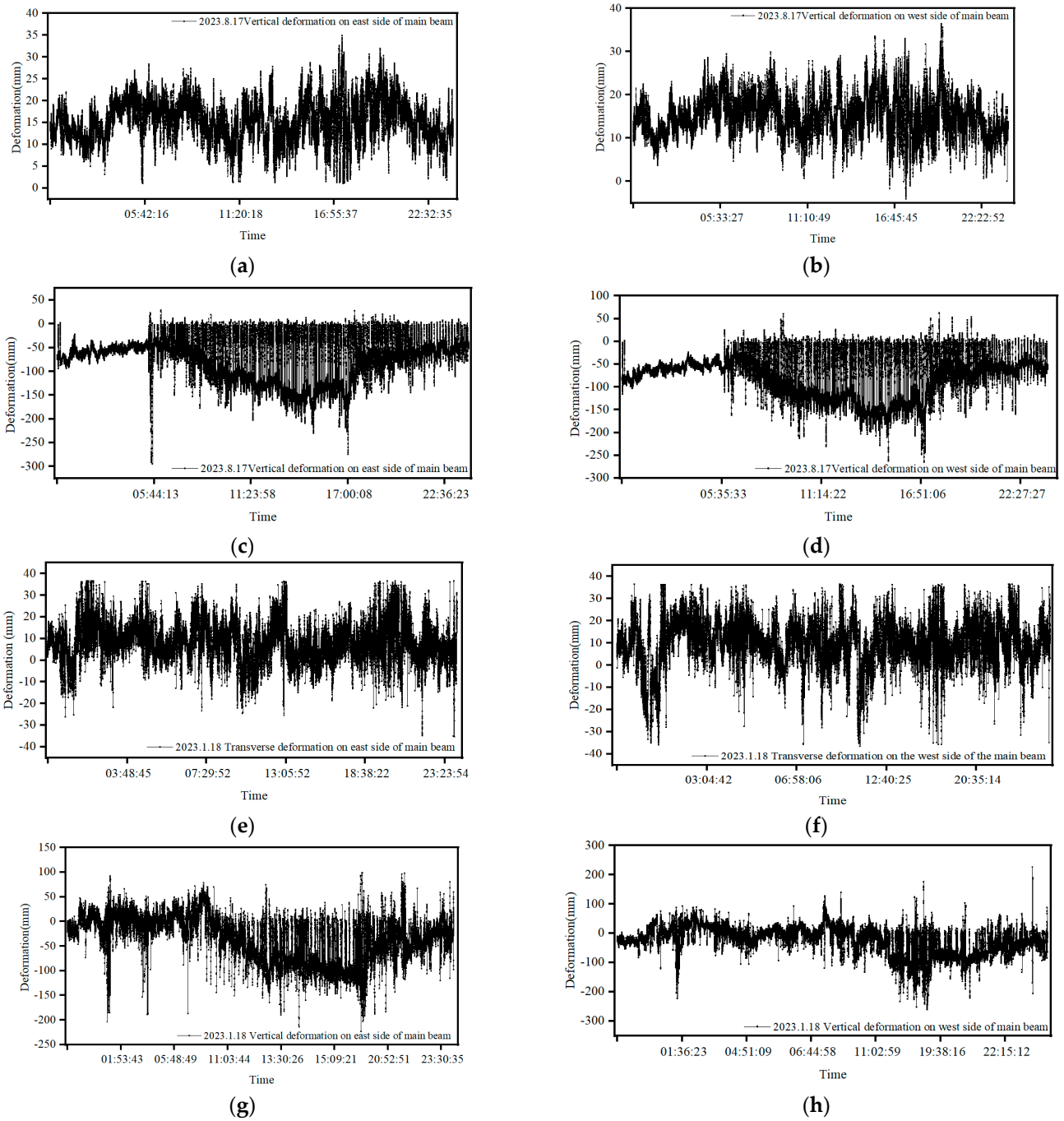

Figure 17. Transverse, vertical and longitudinal deformation of the main beam under temperature load. (**a**) Transverse deformation on 17 August 2023 on the east side of the middle section of the main beam span. (**b**) Transverse deformation on 17 August 2023 on the west side of the middle section of the main beam span. (**c**) Vertical deformation on 17 August 2023 on the east side of the middle section of the main beam span. (**d**) Vertical deformation on 17 August 2023 on the west side of the middle section of the main beam span. (**e**) Transverse deformation on 18 January 2023 on the east side of the middle section of the main beam span. (**f**) Transverse deformation on 18 January 2023 on the west side of the middle section of the main beam span. (**g**) Vertical deformation on 18 January 2023 on the east side of the middle section of the main beam span. (**h**) Vertical deformation on 18 January 2023 on the west side of the middle section of the main beam span.

The temperature has a significant effect on the deformation of the main beam, especially in the vertical deformation. It is found that the deformation of the main beam with

the same section under the action of temperature difference and temperature gradient is far greater than that of a single temperature change under the action of ambient temperature and solar radiation. The high temperature in summer results in thermal expansion of the main beam material, the vertical and transverse deformation increase, and the overall deformation trend is downward. In the coldest winter, the transverse deformation fluctuates around the base point, the degree of change is less than that in summer, and the vertical deformation changes in the same trend, only decreasing in numerical value. Therefore, in the design stage of the bridge, the impact of temperature changes on the material properties should be considered, and enough expansion joints and deformation space should be reserved to adapt to the deformation caused by temperature changes. In the operation and maintenance stage, temperature monitoring should be strengthened to monitor the temperature change in the key parts of the bridge in real time, ensure that the bridge alignment changes within a reasonable range, and provide a scientific guarantee for the safe and stable operation of the train.

6. Conclusions and Discussions

6.1. Conclusions and Prospects

Based on the Chongqing Nanjimen track bridge, this paper analyzes the internal temperature field distribution, transverse temperature distribution and vertical temperature gradient of the steel–concrete composite beam (SCCB), and studies the vertical deformation under the action of the temperature difference and temperature gradient of the system. Moreover, the measured temperature and deformation data of the structure in 2023 are collected and analyzed, and the following conclusions are drawn:

1. The temperature field distribution of steel–concrete composite beams has obvious nonlinearity under the same ambient temperature change. The daily temperature difference is as high as 26 °C, and the internal temperature gradient is significant. The maximum daily temperature difference between the upper and lower edges of the concrete slab is 11.1 °C. Under the influence of solar radiation, the daily transverse temperature gradients of the upper, middle and lower edges of the concrete slab are 3.2 °C, 5.3 °C and 7.4 °C, respectively, due to the thermal insulation effect of the air inside the box girder. Because of its good thermal insulation, the steel beam can adjust the overall temperature change to a certain extent, enhance the adaptability of the structure to the temperature change, and effectively reduce the influence of temperature stress.
2. Under the action of temperature difference and temperature gradient of the system, the overall deformation of the bridge is significant, which affects the alignment of the bridge and the smoothness and comfort of the train. In the context of overall temperature rise, vertical deformation occurs on both sides of the main beam. The maximum deformation of the main beam on the high tower side and the low tower side is 23.9 mm and 92.3 mm, respectively, while the maximum deformation of the mid-span main beam is −63.1 mm. Under the overall cooling effect, the maximum deformation of the main beam at the high tower side and the low tower side is −8.6 mm and −33.3 mm, and the maximum deformation of the mid-span main beam is 22.8 mm. Under the action of positive temperature difference, the maximum deformation of the main beam is 132.1 mm, and the change in the main beam on the low tower side and the high tower side is −7.8 mm and −8.4 mm, respectively. The vertical deformation of the main beam is reversed for negative temperature differences.
3. Temperature has a significant influence on the vertical and lateral deformation of bridges. In the design stage, the impact of temperature changes on material properties should be fully considered, and enough space for expansion joints and deformation should be reserved. In the operation and maintenance stage, temperature monitoring should be strengthened to ensure that the temperature change in key parts is within a reasonable range to ensure the safety of the bridge and the stable operation of the train. Based on the structural temperature and deformation data in 2023, it was found that

the temperature change has a significant impact on the bridge structure. In summer, the high temperature causes the thermal expansion of the material, and the transverse deformation of the main beam reaches the maximum value of 36.4 mm at 16:00, and the vertical deformation reaches the maximum value of −274.4 mm at 15:00. At low temperatures in winter, the transverse deformation changes little and mainly fluctuate around the base point, and the vertical deformation reaches the maximum value of −203.6 mm at 18:00, but the value is lower than that in summer. It is found that the deformation of the main beam with the same section under the action of temperature difference and temperature gradient is far greater than that of a single temperature change under the action of ambient temperature and solar radiation.

This paper examines the impact of temperature on the bridge alignment of a high–low tower superimposed beam track cable-stayed bridge, but further research is required to address the following limitations:

1. COMSOL 6.2 is used to analyze the temperature field of the main beam segment of the Chongqing Nanjimen track bridge. To speed up the calculation speed and improve the calculation efficiency, the track, shear nails and U-shaped ribs and other structures are simplified. In the future, more detailed models will be built to enable more in-depth analysis and research of the bridge structure.
2. The construction time of the Chongqing Nanjimen track bridge is relatively short, the number of temperature monitoring points is limited, and the data collected by the health monitoring system are limited. In the future, more temperature monitoring points will be added and more comprehensive temperature data will be collected for more detailed research and analysis of this type of bridge.

6.2. Discussions

In this paper, the effect of temperature on the shape of long-span steel–concrete superimposed beam track cable-stayed bridge is systematically studied. Through the establishment of numerical models and the analysis of measured data, this study provides valuable information and methods for the in-depth understanding and effective management of the behavior of long-span steel–concrete superposition girder cable-stayed bridges under temperature changes. Although there are some limitations in this study, the results are of great significance for improving the safety management of Bridges, optimizing maintenance strategies, and improving the train driving experience. Future work will focus on further improving the temperature field model, adding more temperature monitoring points and in-depth analysis of the impact of temperature changes on the long-term performance of bridges so as to provide a more accurate basis for bridge health monitoring and maintenance decisions.

Supplementary Materials: The following supporting information can be downloaded at: https://www.mdpi.com/article/10.3390/app142210688/s1, Figure S1: The Chongqing Nanjimen track bridge overall layout; Figure S2: The Chongqing Nanjimen special track bridge structural temperature and deformation system overview.

Author Contributions: X.L.: Conceptualization, validation, writing—review and editing, project administration. X.H.: Investigation, writing—original draft, visualization. P.D.: Methodology, software, validation. X.C.: Resources, data curation, formal analysis. Q.W.: Conceptualization, validation, writing—review and editing. S.C.: Investigation, resources, data curation. All authors have read and agreed to the published version of the manuscript.

Funding: This work was supported by the Chongqing University of Science and Technology Research Grant Program (CKRC2021074) and the China First Highway Engineering Co. R&D project (2024-B-22).

Institutional Review Board Statement: Not applicable.

Informed Consent Statement: Not applicable.

Data Availability Statement: All of the data and models that were generated and used during the study are available from the corresponding author by request. The data are not publicly available due to privacy.

Conflicts of Interest: Authors Peng Ding and Xiaohu Chen were employed by the company T. Y. Lin International Engineering Consulting (China) Co., Ltd. The remaining authors declare that the research was conducted in the absence of any commercial or financial relationships that could be construed as a potential conflict of interest. The authors declare that this study received funding from China First Highway Engineering Co. The funder was not involved in the study design, collection, analysis, interpretation of data, the writing of this article or the decision to submit it for publication.

References

1. Li, X.; Gao, M.; Zhou, J.; Chen, X.; Tan, S. Permanent deformation limits of long-span track cable-stayed bridges based on service performance analysis. *J. Low Freq. Noise Vib. Act. Control* **2021**, *40*, 1215–1226. [CrossRef]
2. Mansour, W.; Tayeh, B.A.; Tam, L.-H. Finite element analysis of shear performance of UHPFRC-encased steel composite beams: Parametric study. *Eng. Struct.* **2022**, *271*, 114940. [CrossRef]
3. Huang, Z.; Wei, Y.; Zhang, Y.; Zhao, K.; Dong, Z. Flexural performance of FRP-SWSSC-steel composite beams: Experimental and analytical investigation. *Eng. Struct.* **2024**, *306*, 117842. [CrossRef]
4. Zhou, Y.; Uy, B.; Wang, J.; Li, D.; Huang, Z.; Liu, X. Behaviour and design of stainless steel-concrete composite beams. *J. Constr. Steel Res.* **2021**, *185*, 106863. [CrossRef]
5. Guo, Y.-T.; Yang, Y.; Song, S.-Y.; Fan, J.-S. Shear–slip failure in steel–concrete–steel composite beams with bidirectional webs. *Thin-Walled Struct.* **2021**, *164*, 107743. [CrossRef]
6. Xie, X.; Su, H.; Pang, M. Mechanical Properties and Experimental Study of a New Laminated Girder Single Tower Cable-Stayed Bridge. *Int. J. Steel Struct.* **2023**, *23*, 872–8851. [CrossRef]
7. Sun, T.; Yang, J.; Jing, Z.; Zhou, S. Research and application of construction method for long span steel-concrete composite beam bridge. In *Constructional Engineering and Ecological Environment*; CRC Press: Boca Raton, FL, USA, 2023; pp. 114–119.
8. Nilimaa, J.; Hösthagen, A.; Emborg, M. Thermal crack risk of concrete structures: Evaluation of theoretical models for tunnels and bridges. *Nord. Concr. Res.* **2017**, *56*, 55–69.
9. Tan, H.; Qian, D.; Xu, Y.; Yuan, M.; Zhao, H. Analysis of Vertical Temperature Gradients and Their Effects on Hybrid Girder Cable-Stayed Bridges. *Sustainability* **2023**, *15*, 1053. [CrossRef]
10. Zhang, Q.; Cai, X.; Zhang, Y.; Wang, T.; Zhong, Y. Real-time temperature field and thermal deformation of slab track on cable-stayed bridge. *Case Stud. Therm. Eng.* **2023**, *51*, 103582. [CrossRef]
11. Davoodnabi, S.M.; Mirhosseini, S.M.; Shariati, M. Analyzing shear strength of steel-concrete composite beam with angle connectors at elevated temperature using finite element method. *Steel Compos. Struct. Int. J.* **2021**, *40*, 853–868.
12. Mo, J.; Uy, B.; Li, D.; Thai, H.-T.; Tran, H. A review of the behaviour and design of steel–concrete composite shear walls. *Structures* **2021**, *31*, 1230–1253. [CrossRef]
13. Ellobody, E. *Finite Element Analysis and Design of Steel and Steel-Concrete Composite Bridges*; Elsevier: Amsterdam, The Netherlands, 2023.
14. Li, X.; Luo, H.; Ding, P.; Chen, X.; Tan, S. Prediction Study on the Alignment of a Steel-Concrete Composite Beam Track Cable-Stayed Bridge. *Buildings* **2023**, *13*, 882. [CrossRef]
15. Zhou, H.; Yi, Y.L.; Ye, Z.T.; Li, M. Analysis of temperature filed and thermal effect in long-span composite girder cable-stayed bridge. *Bridge Constr.* **2020**, *50*, 50–55.
16. Zhou, Y.; Sun, L.-M.; Fu, Z.-H.; Jiang, Z. Studyon Temperature Sensitivity Coefficients of Mid-Span Vertical Displacement of Cable-Stayed Bridges. *Eng. Mech.* **2020**, *37*, 148–154.
17. Zhou, Y.; Sun, L.-M.; Xie, M.-W. Temperature effects on the mid-span vertical displacement of a cable-stayed bridge. *Eng. Mech.* **2018**, *35*, 46–54.
18. Yang, J.-N.; He, X.-J.; Yang, J.-H.; Wang, Y.-D.; Zhang, C. Analysis of Temperature Effect on an S Cable-Stayed Bridge with Steel BoxGirder During Asphalt Concrete Placement. *Bridge Constr.* **2020**, *50*, 37–42.
19. Huang, Q.; Zhao, D.Y.; Ren, Y.; Xu, X. Multiple time scale analysis of temperature-induced deflection of cable-stayed bridges. *J. Harbin Inst. Technol.* **2020**, *52*, 18–25.
20. Liu, Y.-F.; Zhao, H.-S.; Wang, R.-G.; Wei, L.-Y.; Nie, X.; Fan, J.-S. Research on Temperature Effect of Composite Bridge Tower in Zhang-JingGao Yangtze River Bridge Under Solar Radiation. *China J. Highw. Transp.* **2024**, *37*, 125–136.
21. Zhao, Y.; Zhang, Y.-J.; Zhou, Y.; Wan, J.-B.; Li, R.-R. Analysis of Temperature Effect of Earth-Anchored Single Inclined PylonCable-Stayed Bridge with a Universal Hinge. *Bridge Constr.* **2021**, *51*, 54–61.
22. Zhou, R.; Yuan, W.; Zhu, X.; Liu, H.; Yang, H.; Wang, Y. Temperature Effect Analysis of CRTS II Ballastless Track with Different.Substructures. *J. Railw. Eng. Soc.* **2023**, *40*, 13–20+61.
23. Zhu, Y.; Sun, D.; Guo, H.; Shuang, M. Fine analysis for non-uniform temperature field and effect of railway truss suspension bridge under solar radiation. *J. Constr. Steel Res.* **2023**, *210*, 108098. [CrossRef]

24. Sousa Tomé, E.; Pimentel, M.; Figueiras, J. Structural response of a concrete cable-stayed bridge under thermal loads. *Eng. Struct.* **2018**, *176*, 652–672. [CrossRef]
25. Abid, S.R.; Xue, J.; Liu, J.; Tayşi, N.; Liu, Y.; Özakça, M.; Briseghella, B. Temperatures and gradients in concrete Bridges: Experimental, finite element analysis and design. *Structures* **2022**, *37*, 960–976. [CrossRef]
26. Cai, D.; Shi, Y.; Lou, L.; Yan, H.; Lv, S. Research on Temperature Field Characteristics of Subgrade Structure with Asphalt Concrete Surface for Ballast Track. *J. China Railw. Soc.* **2022**, *44*, 64–71.
27. Kang, W.; Chen, S.; Wei, C.; Liu, X.; Li, J. Temperatures of Ballastless Track and Effect of Continuous Hot Weather. *J. China Railw. Soc.* **2019**, *41*, 127–134.
28. *GBT51234-2017*; Code for Design of Urban Rail Transit Bridge. 5.2 Load Value. China Architecture & Building Press: Beijing, China, 2017. Available online: https://ebook.chinabuilding.com.cn/zbooklib/bookpdf/probation?SiteID=1&bookID=98209 (accessed on 13 November 2024).
29. Li, X.; Huang, X.; Ding, P.; Wang, Q.; Wang, Q. Research on an Intelligent Identification Method for Cable-Stayed Force with a Damper Based on Microwave Radar Measurements. *Buildings* **2024**, *14*, 568. [CrossRef]
30. Zhang, Q.; Cao, W.; Dai, G. Analysis of temperature field of concrete slab under solar radiation. *Build. Struct.* **2023**, *53*, 1728–1732.
31. Dai, G.; Zhang, Q.; Ge, H.; Rao, H. Research on thermal field of concrete box girder based on integratransformation method. *J. Huazhong Univ. Sci. Technol. (Nat. Sci. Ed.)* **2021**, *49*, 77–82.
32. Wang, Z.; Liu, Y.J.; Tang, Z.W.; Zhang, G.J.; Liu, J. Three-dimensional temperature field simulation method of truss arch rib based on sunshine shadow recognition. *China J. Highw. Transp.* **2022**, *35*, 91–105.
33. Gou, H.; Chen, Z.; Liu, C.; Xiao, C.; Yuan, W.; Su, Y. Thermal Field of Composite Girder-Ballastless Track System on Arch inPlateau and Regions with Large Diurnal Temperature Variation Based onMeasured Data. *J. China Railw. Soc.* **2023**, *46*, 159–170.
34. Ding, P.; Li, X.; Chen, S.; Huang, X.; Chen, X.; Qi, Y. Load Effect Analysis Method of Cable-Stayed Bridge for Long-Span Track Based on Adaptive Filtering Method. *Appl. Sci.* **2024**, *14*, 7057. [CrossRef]